Aluminum nanoscale order in amorphous $Al_{92}Sm_8$ measured by fluctuation electron microscopy

W. G. Stratton, J. Hamann, J. H. Perepezko, and P. M. Voyles[a)]
Department of Materials Science and Engineering, University of Wisconsin—Madison, Madison, Wisconsin 53706

X. Mao
Department of Physics, University of Illinois—Urbana Champaign, Urbana, Illinois 61801

S. V. Khare[b)]
Department of Materials Science and Engineering, University of Illinois—Urbana Champaign, Urbana, Illinois 61801

Fluctuation electron microscopy (FEM) measurements and simulations have identified nanoscale aluminum-like medium-range order in rapidly quenched amorphous $Al_{92}Sm_8$ which devitrifies by primary Al crystallization. $Al_{92}Sm_8$ amorphized by plastic deformation shows neither Al nanoscale order, nor primary crystallization. Annealing the rapidly quenched material below the primary crystallization temperature reduces the degree of nanoscale Al order measured by FEM. The FEM measurements suggest that 10–20 Å diameter regions with Al crystal-like order are associated with primary crystallization in amorphous $Al_{92}Sm_8$, which is consistent with the quenched-in cluster model of primary crystallization. © *2005 American Institute of Physics.* [DOI: 10.1063/1.1897830]

High-Al content amorphous alloys[1] are of interest due to their high tensile strength and unusual devitrification behavior. Devitrification of rapidly quenched amorphous $Al_{92}Sm_8$ at $<250\ °C$ produces pure Al nanocrystals at concentrations $>10^{21}\ m^{-3}$.[2,3] Devitrification of $Al_{92}Sm_8$ amorphized by deformation does not proceed by primary Al crystallization.[3] When annealed below T_g, the melt-spun material exhibits a steadily decreasing nucleation rate,[4] which suggests heterogeneous nucleation.[5] The nucleation site has so far eluded structural or chemical detection, ruling out common sites like second phase interfaces or large impurity clusters. This suggests that the nucleation sites in quenched $Al_{92}Sm_8$ may be a form of nanometer-length structure or medium-range order (MRO). Such structure is difficult to detect in amorphous materials using conventional techniques such as x-ray diffraction.[6] Here, we report fluctuation electron microscopy (FEM) (Refs. 7 and 8) measurements and simulations which find MRO associated with primary crystallization in amorphous $Al_{92}Sm_8$.

FEM measures diffraction from nanoscale volumes using dark-field transmission electron microscopy (TEM) at a deliberately low (5–50 Å) image resolution. The magnitude of the spatial fluctuations in diffraction, measured by the normalized variance V as a function of scattering vector k, gives information about MRO at the length scale of the image resolution.[7,9] $V(k)$ depends on the three- and four-body atomic position correlation functions.[9] Peaks in $V(k)$ give information about the type of MRO from their position in k and the degree of MRO from their height. A polycrystalline sample is an extreme example of order: in a dark-field image each grain will appear brightest when it satisfies a Bragg condition in k, leading to a high peaks in $V(k)$ at the crystal reciprocal lattice k's.

Samples of amorphous $Al_{92}Sm_8$ were prepared by rapid quenching in a single wheel melt spinner at a tangential wheel speed of 55 m/s and by cold-rolling elemental foil multilayers at a $0.003\ s^{-1}$ strain rate. Melt-spun ribbon samples were annealed at 130 °C ($<T_g$ of 171 °C)[3,10] under vacuum. TEM samples were prepared by electropolishing only, as ion milling can introduce spurious peaks in $V(k)$ of amorphous metals.[11] FEM was done in hollow-cone dark-field mode on a LEO 912 EFTEM at 120 kV and 16 Å resolution. Each $V(k)$ data set is the mean of measurements from at least seven areas of the sample, quoted with one standard deviation of the mean error bars.
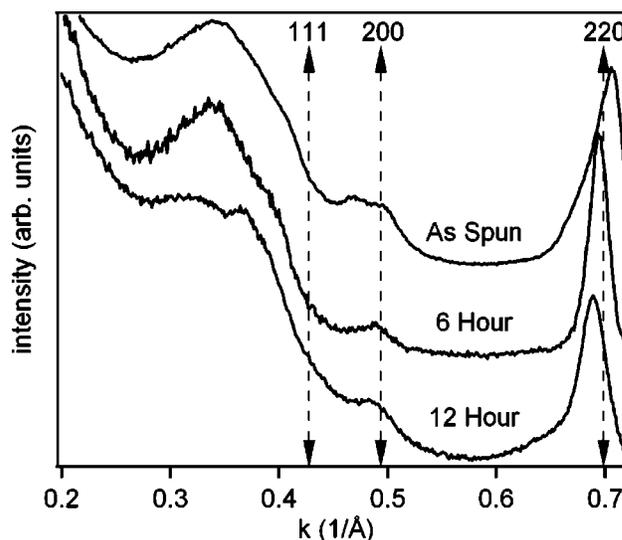

FIG. 1. The annular average of electron diffraction patterns from melt-spun $Al_{92}Sm_8$ samples as spun and after 6 and 12 h anneals. The patterns have been shifted vertically for clarity, and the vertical lines indicate the face-centered-cubic Al $\langle 111 \rangle$, $\langle 200 \rangle$, and $\langle 220 \rangle$ reflections.

[a)]Author to whom correspondence should be addressed; electronic mail: voyles@engr.wisc.edu
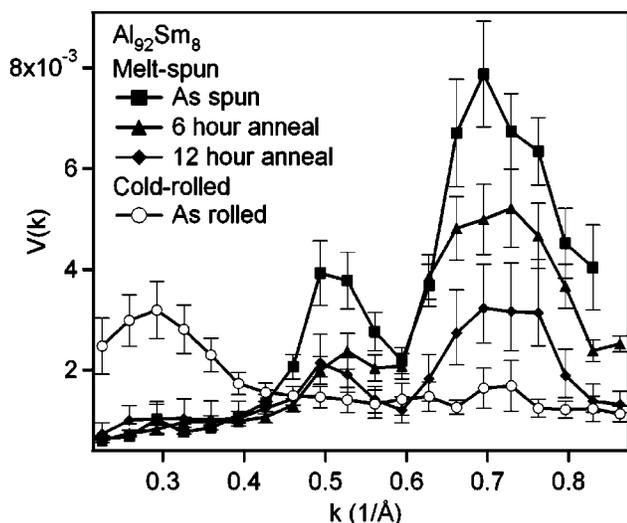[b)]Current address: Department of Physics, University of Toledo, Toledo, OH 43606.

FIG. 2. Fluctuation microscopy data $V(k)$ for melt-spun as spun, 6, and 12 h annealed, and cold-rolled $Al_{92}Sm_8$.

Figure 1 shows the annular average of electron diffraction patterns, which measure short-range order, from the MSR as a function of annealing. Peaks occur at the Al $\langle 200 \rangle$ and $\langle 220 \rangle$ positions, but not the $\langle 111 \rangle$. The broad maximum below 0.4 Å^{-1} covers several reflections in various Al–Sm intermetallic phases, suggesting it is associated with Al–Sm distances. Annealing produces some small changes in the short-range order. The shifts in the $\langle 220 \rangle$ peak could be due to ~1% strains, but they are probably due to drift in the TEM camera length. The change in shape of the low k peak after 12 h of annealing is more likely to be meaningful and may indicate some structural relaxation.

The MSR $V(k)$ shown in Fig. 2 arises from nanoscale Al-like order in the sample. The peaks at 0.5 and 0.7 Å^{-1} correspond to the Al $\langle 200 \rangle$ and $\langle 220 \rangle$ reflections. The second peak also covers the Al $\langle 311 \rangle$ at 0.82 Å^{-1}. Figure 3 shows $V(k)$ simulated for both a 30 Å diameter crystalline Al sphere and icosahedron of 12 Al atoms surrounding a Sm atom[12] using an extension of the Dash *et al.*[13] method to binary

systems. The Al model reproduces both the peak positions and the relative peak heights in the MSR $V(k)$. Icosehedron and $Al_{11}Sm_3$ and Al_4Sm sphere simulations (not shown) fail to reproduce even the experimental peak positions.

We describe this structure as "Al-like order" because these simulations are not a full atomistic model for the material. They involve only the basic motifs that dominate $V(k)$.[14] Nor is a 30 Å crystalline Al sphere unique in approximating the data; simulations for smaller spheres containing one to two substitutional Sm atoms match almost as well. Slightly different crystal sizes, shapes, or orientation distributions are also likely to be broadly consistent with the data. What is required is diffraction from some Al Bragg condition that is spatially heterogeneous on a length scale of 16 Å, the spatial resolution of the imaging. This means atoms locally organized into an fcc Al lattice (possibly strained, distorted, or impure); thus "nanoscale Al-like order."

The structural origin of the peak at 0.3 Å^{-1} in the cold-rolled $V(k)$ is not clear. It is not an Al reflection, and while it could be an intermetallic or icosehedral reflection, simulations of those structures show peaks at higher k not seen in the data. Modeling this result will be the subject of future work.

As with most TEM measurements on amorphous materials, we must be concerned with electron beam damage to our samples. Diffraction and $V(k)$ both show discernable changes after 10 min exposure under our experimental conditions. The FEM data in Fig. 2 took ~20 min to acquire scanning from low to high k, so the points at $k > 0.65$ Å^{-1} will have some beam damage. We believe our conclusions remain valid for three reasons. First, the as-spun $V(k)$ for $k = 0.6 – 0.8$ Å^{-1} has been reproduced with 4 min exposure. Second, the beam-induced change in $V(k)$ is similar in magnitude to the area-to-area variability represented by the errors bars in Fig. 2. Third, the exposures for each data set are similar, so differences in $V(k)$ upon annealing are not beam-damaged induced.

Our data support the model that primary crystallization in these alloys is driven by crystal Al clusters formed during the quench, then frozen into the structure.[2,3,15] At a given annealing temperature, some of those clusters are supercritical and grow into stable crystals, which predicts the observed decrease in nucleation rate under isothermal annealing.[4] Figure 2 shows that the degree of MRO, indicated by the height of the peaks,[16] is reduced by the same isothermal anneal. If the sample is crystallizing, why do we measure *less* order? A single large crystal in the field of view will dominate the $V(k)$ signal from the surrounding material, so we avoid them when making FEM measurements. That means that in the annealed samples, we measure the remaining population of clusters, not the crystallized material. Moreover, based on the final nanocrystal density, we estimate that there are on order of ten supercritical clusters per 0.3×0.3 μm micrograph. Particle analysis of the micrograph shows, however, that $V(k)$ is not due to a few bright features; rather there are a range of feature sizes and intensities. This precludes a sharp delineation in intensity between clusters and matrix, but it suggests that FEM is sensitive to the smaller subcritical frozen-in clusters that are formed at very high density during the quench. These subcritical clusters relax upon annealing, leading to a less-ordered average structure between the stable crystals, exactly as observed in Fig. 2.
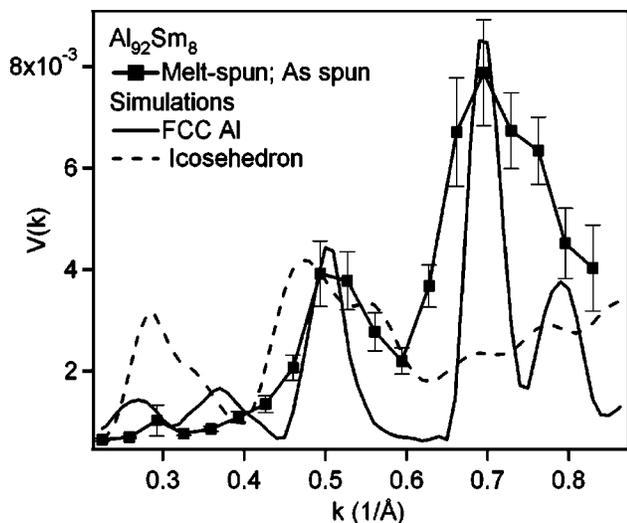

FIG. 3. Measured $V(k)$ for melt-spun as spun and simulated $V(k)$ for a 30 Å Al sphere and a Sm-centered icosahedron. The Al sphere reproduces the peak positions and relative heights. The simulations have been multiplicatively scaled to match the data.

We can therefore bracket the critical cluster size in this alloy: It must be small enough not to appear in conventional TEM, so <30 Å, but large enough to generate a significant FEM signal. The maximum $V(k)$ will come from particles the size of the resolution (16 Å)[17] so we put the low limit at ~10 Å. Separate analysis based on crystallization kinetics and nucleation densities indicates critical cluster sizes in the range of 8–15 Å (Ref. 18) which is close to previous estimates[19] and represents a satisfactory consistency. More accurate measurements of the cluster size distribution require systematic variable resolution FEM.[9]

Other hypotheses have been advanced to explain primary crystallization. We see no evidence for amorphous phase separation.[20] Xing *et al.*[21] have suggested that some high Al-content amorphous alloys are not glasses, but instead amorphous-nanocrystal composites, and that primary crystallization is grain coarsening, not a phase transition. Our observation of nanoscale Al order in the as-spun ribbon is consistent with this model, but the *decrease* of that order with annealing may not be.

In summary, FEM measurements have discovered Al-like nanoscale order in melt-spun amorphous $Al_{92}Sm_8$. Cold-rolled glass of the same composition shows different nanoscale order, and the order in the spun alloy decreases with annealing treatments. Our data support the quenched-in cluster model of primary crystallization.[2,3,15]

[1] A. Inoue, K. Ohtera, A. P. Tsai, H. Kimura, and T. Masumoto, Jpn. J. Appl. Phys., Part 2 **27**, L1579 (1988); Y. He, S. J. Poon, and G. J. Shiflet, Science **241**, 1640 (1988).

[2] J. C. Foley, D. R. Allen, and J. H. Perepezko, Scr. Mater. **35**, 655 (1996).

[3] G. Wilde, H. Sieber, and J. H. Perepezko, Scr. Mater. **40**, 779 (1999).

[4] G. Wilde, H. Rosner, N. Boucharat, J. Hamann, W. S. Tong, and J. H. Perepezko, *Proceedings of the Materials Research Society*, Boston, MA, **806**, 33–38 (2003).

[5] S. K. Das, J. H. Perepezko, R. I. Wu, and G. Wilde, Mater. Sci. Eng., A **304**, 159 (2001).

[6] J. M. Gibson and M. M. J. Treacy, Phys. Rev. Lett. **78**, 1074 (1997).

[7] M. M. J. Treacy and J. M. Gibson, Acta Crystallogr., Sect. A: Found. Crystallogr. **52**, 212 (1996).

[8] P. M. Voyles, J. M. Gibson, and M. M. J. Treacy, J. Electron Microsc. **49**, 259 (2000).

[9] J. M. Gibson, M. M. J. Treacy, and P. M. Voyles, Ultramicroscopy **83**, 169 (2000).

[10] J. H. Perepezko and R. J. Hebert, JOM **54**, 34 (2002).

[11] J. Li, X. Gu, and T. C. Hufnagel, Microsc. Microanal. **9**, 509 (2003).

[12] L. Cervinka, J. Non-Cryst. Solids **156**, 94 (1993).

[13] R. K. Dash, P. M. Voyles, J. M. Gibson, M. M. J. Treacy, and P. Keblinski, J. Phys.: Condens. Matter **15**, S2425 (2003).

[14] S. V. Khare, S. M. Nakhmanson, P. M. Voyles, P. Keblinski, and J. R. Abelson, Appl. Phys. Lett. **85**, 745 (2004).

[15] K. Nakazato, Y. Kawamura, A. P. Tsai, and A. Inoue, Appl. Phys. Lett. **63**, 2644 (1993).

[16] P. M. Voyles, N. Zotov, S. M. Nakhmanson, D. A. Drabold, J. M. Gibson, M. M. J. Treacy, and P. J. Keblinski, J. Appl. Phys. **90**, 4437 (2001).

[17] P. M. Voyles and J. R. Abelson, Sol. Energy Mater. Sol. Cells **78**, 85 (2003).

[18] J. H. Perepezko and J. Hamann (unpublished).

[19] J. C. Foley, D. R. Allen, and J. H. Perepezko, Scr. Mater. **35**, 655 (1996).

[20] A. K. Gangopadhyay, T. K. Croat, and K. F. Kelton, Acta Mater. **48**, 4035 (2000); K. F. Kelton, T. K. Croat, A. K. Gangopadhyay, L.-Q. Xing, A. L. Greer, M. Weyland, X. Li, and K. Rajan, J. Non-Cryst. Solids **317**, 71 (2003).

[21] L. Q. Xing, A. Mukhopadhyay, W. E. Buhro, and K. F. Kelton, Philos. Mag. Lett. **84**, 293 (2004).